GKSS
FORSCHUNGSZENTRUM
in der HELMHOLTZ-GEMEINSCHAFT

Final Draft
of the original manuscript:

Prado, L.A.S.de A.; Ponce, M.L.; Goerigk, G.; Funari, S.S.; Haramus, V.; Willumeit, R.; Schulte, K.; Pereira Nunes, S.:

Analysis of proton-conducting organic–inorganic hybrid materials based on sulphonated poly(ether ether ketone) and phosphotungstic acid via ASAXS and WAXS

In: Journal of Non-Crystalline Solids (2008) Elsevier

DOI: 10.1016/j.jnoncrysol.2008.09.036

Analysis of proton-conducting organic-inorganic hybrid materials based on sulphonated poly(ether ether ketone) and phosphotungstic acid via ASAXS and WAXS.

Luis Antonio Sanchez de Almeida Prado[1*], Mariela L. Ponce[2], Günter Goerigk[3], Sérgio S. Funari[4], Vasyl M. Garamus[2], Regine Willumeit[2], Karl Schulte[1] and Suzana Pereira Nunes[2].

[1]Institut für Kunststoffe und Verbundwerkstoffe - TUHH, Denickerstraße 15, D-21073 Hamburg, Germany

[2]GKSS Research Centre Geesthacht GmbH, Max-Planck-Straße 1, D-21502 Geesthacht, Germany

[3]Institute of Solid State Research, Research Center Jülich, P.O. Box 1913, D-52425, Jülich, Germany

[4] Hasylab at DESY, Notkerstraße 85, D-22067, Hamburg, Germany

*Corresponding author:

Dr. L. A. S. de A. Prado

Technical University Hamburg-Harburg

Denickestraße 15

D-21073 Hamburg

Germany

E-mail L.Prado@tuhh.de,

Fax +49 40 42878 2002 Tel: +49 40 42878 4136

1. Introduction

Polyelectrolytes have gained considerable attention on account of their potential application as membranes for polyelectrolyte membrane fuel cell PEMFCs [1-3]. In this context, a lot of work has been done in order to synthesize polymers and copolymers bearing sulfonic and/or phosphonic groups due to their good proton-conductivity [1-12]. When methanol is used as fuel, the desired properties such as low methanol cross-over, high proton-conductivity can just be achieved through the preparation of organic-inorganic hybrid material or nanocomposites. In this context inorganic proton-conductors such as heteropolyacids [3,13-16], zirconium phosphates [17-20] play an important role in increasing the proton-conductivity of polymeric matrices such as poly(benziimidazole) [21-22], sulphonated poly(arylene ether ketone) SPEK [14], sulphonated poly(arylene ether ether ketone) SPEEK[15,19,20], sulphonated poly(arylene ether sulfone) [13] among others [23].
Usually the heteropolyacids are used in combination with *in situ* generated ZrO_2 or polysilsesquioxanes, in order to avoid the bleeding-out of the heteropolyacid during the membrane operation in the PEMFCs [14,15]. To our knowledge a little amount of work has been carried out in order to analyze the distribution of heteropolyacids or other inorganic additives in such multi-component organic-inorganic hybrid materials [24-26]. Previous results from our group, have demonstrated that the distribution of heteropolyacids in ionomers depends strongly on the nature of the ionomer, heteropolyacid and additives. These additives affect the distribution, crystallization and fixation of heteropolyacids by the membrane. In this context, the goal of the present investigation is to analyze the distribution of phosphotungstic acid in SPEEK matrix in the presence of different additives.

2. Anomalous Small-Angle X-ray Scattering [27-34]

Small-Angle X-ray Scattering is an already established technique for the analysis of the morphology and microstructure of several materials. Due to fluctuations of electron density the scattered X-rays give rise to characteristic patterns. The scattering intensity I(q) is usually plotted as a function of the scattering vector q, which is defined by the equation (1).

$$q = \frac{4\pi}{\lambda}\sin\left(\frac{\theta}{2}\right) \quad (1)$$

where θ and λ correspond to the scattering angle and the wave-length of the incident X-rays.

More precise information concerning the scattering produced by a sample can be obtained by varying the energy of the incident X-ray in order to approach the absorption edge of an element present in the sample. Because the scattering power of the element is strongly attenuated at these energies the intensity of the scattering curves should change, if the scatters contain an element which absorbs the X-ray at that specific energy. [32,33]

This specific variant of the SAXS technique, termed anomalous (or resonant) small-angle X-ray scattering (ASAXS), has been successfully used for the morphological characterization of polymers bearing ionic groups, such as: Surlyn-ionomers, polyelectrolyte brushes [34] and most recently organic-inorganic hybrids based on sulphonated poly(ether ketone) and sulphonated poly(ether ether ketone).

When dealing with very diluted scatterers, the Guinier approximation can provide information about their size and shape. Assuming a relative mono-disperse distribution of spherical scatteres diluted in a matrix, the radius of the scatterers (R) can be estimated from the Guinier gyration radius (R_g), using the equations (2) and (3).

$$I(q) \propto \exp -\left(\frac{-Rg^2 \times q^2}{3} \right) \quad (2)$$

$$R = Rg\sqrt{\frac{5}{3}} \quad (3)$$

If the Guinier approximation holds for the system under anaylsis, the curve of logarithm of the intensity as a function of q^2 should be linear. The R_g can be determined from the slope of the segment observed in the q-range between the scattering vector values q_1 and q_2. Furthermore, the validity of the Guinier approximation is useful if the condition shown in equation (4) is satisfied.[35]

$$q_2{}^2 \times Rg^2 < (1.3)^2 \quad (4)$$

When dealing with ASAXS curves, the analysis of the scattering pattern using the Guinier approximation is particularly convenient, as at low q-values the intensity of the scattered X-ray is usually much higher than the fluorescence and residual Raman scattering, which are produced when the sample is irradiated with X-rays having energy close to the absorption edge of a component of the material under analysis.

3. Experimental

3.1. Materials.

Zirconium tetrapropylate was supplied as a 70% solution in 1-propanol (Aldrich); phosphotungstic acid, PTA, ($H_3PW_{12}O_{40}.xH_2O$) and acetylacetone were provided by Fluka and were used without previous purification. N-methylpirrolidone, NMP, was used as solvent for the membrane manufacturing. The 3-aminopropyltrimethoxysilane was supplied by Aldrich. Sulfonated poly(ether ether ketone) with a sulfonation degree of 66-67%, SPEEK, was obtained in the laboratory by the sulfonation of PEEK 450P, supplied in pellets by Victrex, using a procedure described previously [20].

3.2. SPEEK/PTA membranes.

SPEEK/PTA membranes were cast from solutions containing about 7 wt% of SPEEK in DMF. The required amount of PTA was added to these solutions and stirred for 24h at least at room temperature. The final composition of the material was SPEEK/PTA 63/37 (w/w)

3.3. SPEEK/$(RSiO_{3/2})_n$/PTA and SPEEK/ZrO_2/PTA membranes.

The alkoxide and small amounts of water (about 4.5 mol water/mol of amino silane or zirconium propylate) were added to the polymer solution of SPEEK and stirred during 2 hours at 50^{o}C to complete the hydrolysis and condensation of the alkoxide. The final material contained 9 wt % poly(3-amimopropylsilsesquioxane) in the polymer matrix. Following the same procedure, membranes were prepared with the following

compositions: SPEEK/ZrO_2 92/8 (w/w), SPEEK/ZrO_2/PTA 64/8/28 (w/w/w); and SPEEK/$(RSiO_{3/2})_n$/PTA 61/2/37 (w/w/w).

3.4. Casting of the membranes.

All the solutions containing SPEEK and the inorganic component were cast on a hydrophobic glass plate heated to temperatures ranging from 40^o to 90^{o}C for solvent evaporation.

3.5. WAXS Experiments.

The WAXS experiments were carried out at the Soft Condensed Matter beamline A2 at HASYLAB, Hamburg, with a fixed wavelength of 1.5 Å under vacuum at room temperature. The WAXS data were calibrated using the characteristics reflections of a poly(ethylene terephtalate) (PET) film. Corrections due to the parasitic scattering (background) were done after measurement of each sample [25].

3.6. ASAXS Measurements.

The ASAXS measurements were performed at the JUSIFA beamline at DESY-HASYLAB, Hamburg[36]. In order to use the anomalous scattering of tungsten for contrast variation, four different X-ray energies were used in the energy range of the W-L_{III} edge at 10206 eV: 9678 eV (E1), 10131 eV (E2), 10196 eV (E3) and 10206 eV (E4). Two sample-detector distances (935 and 3635 mm) were set up in order to cover a wide q-range between 0.02 and 0.5 Å^{-1}. The scattering curves were calibrated into macroscopic scattering cross-sections in units of cross-section per unit

volume [$cm^2/cm^3 = cm^{-1}$]. Background scattering due to fluorescence and thermal fluctuations was removed using the Porod-like approximation.[24,37]

4. Results

Fig. 1 displays the total scattering curves produced by the SPEEK/PTA membrane. As expected for a two-phase system, the intensity decreases as the energy of the incident X-ray approaches the W-L_{III} absorption edge, due to the attenuation of the scattering power of this element at energy values close to an absorption edge. The decrease of the intensity is an indicative of the higher electron-density of the PTA in comparison to the polymeric SPEEK matrix.

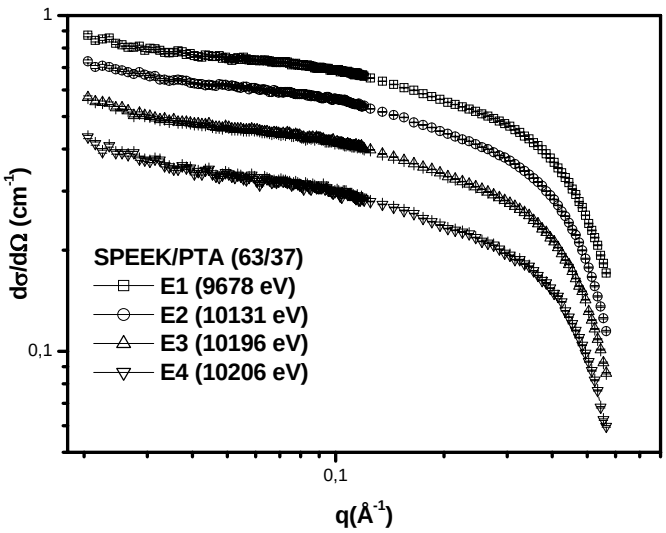

Fig.1 Total scattering curves of SPEEK/PTA membranes.

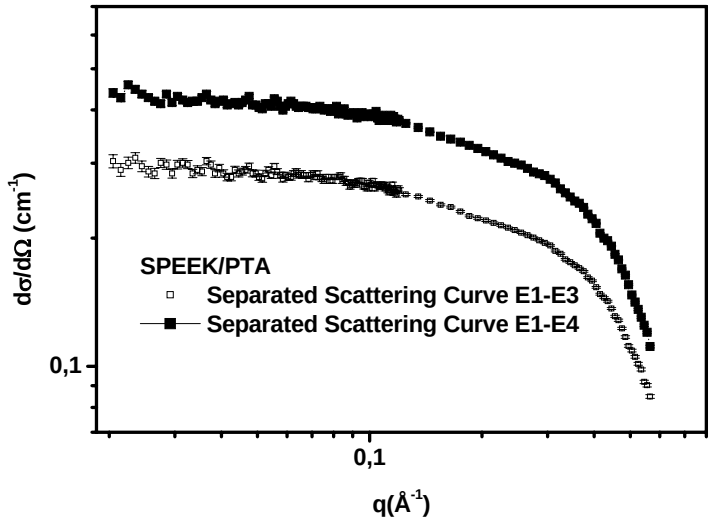

Fig. 2. Separated scattering curves produced by SPEEK/PTA membrane. These curves were obtained by subtracting the total scattering curve at E1 (9678 eV) from those measured at E4 (10206 eV) or E3 (10196 eV)

As can be seen in Fig.2, the separated scattering curves are parallel at q lower than 0.35 $Å^{-1}$. At higher q-values, the parasitic contribution of the fluorescence may not be completely removed, therefore the data at very high q-values should contain some artifacts, which stems from an imprecise subtraction of the background. At lower q-values, the intensity of the scattering is much higher than at high q-values. Therefore, the relative effect of the fluorescence should not be so important in this case.

At very small q-values, the Guinier approximation could be used in order to determine the gyration radius (R_g) of the PTA scatterers. The resulting Guinier plots are displayed in Fig. 3. Two separated scattering curves were analyzed for comparison. In both cases, a straight line segment was observed, from which R_g and the size of the scatterers (R) could be estimated, according to the theory described in the introduction of the present paper. Very similar R_g and R values, around 5.0 Å and 6.5

Å, respectively, were obtained from both curves, indicating that at this range the separated curves are reliable and represent a two-phase system composed by PTA dispersed in SPEEK matrix. Moreover, as the radius of the isolated PTA anion is around 5.0 Å [38], the analysis of the ASAXS curve demonstrated the existence of a solid solution of PTA dissolved in the SPEEK matrix.

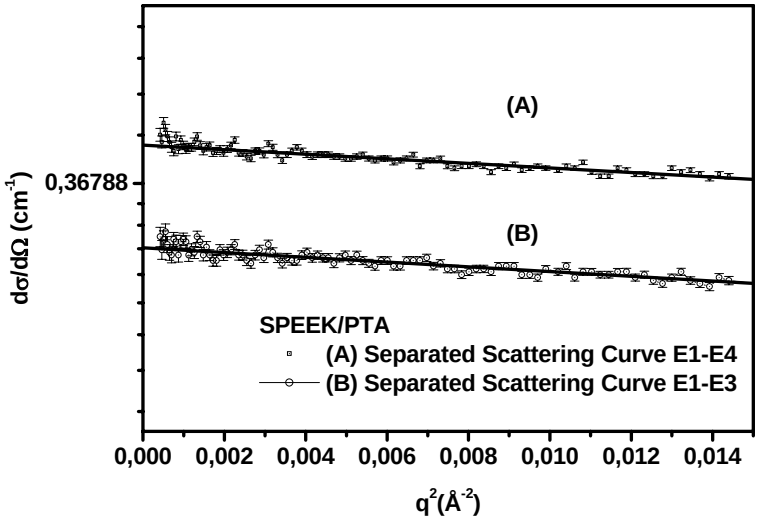

Fig. 3. Guinier plots for SPEEK/PTA membranes obtained from the separated scattering curves illustrated in Fig. 2.

The possibility of crystallization of the heteropolyacid during the casting of the membrane was checked out by the analysis of the WAXS pattern of the SPEEK/PTA membrane, which is reported in Fig. 4.

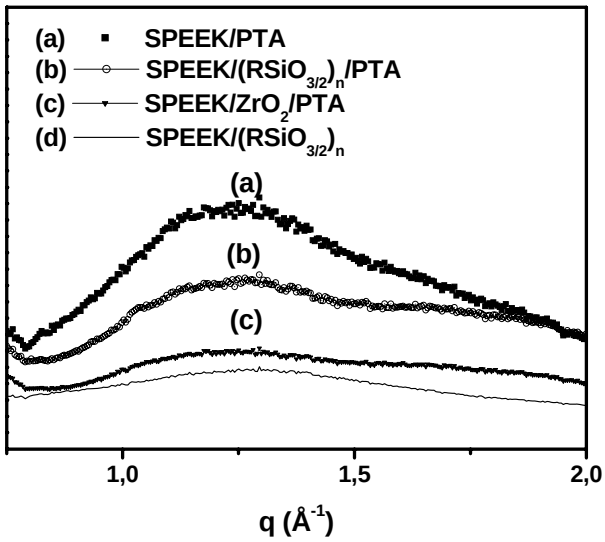

.

Fig. 4. WAXS patterns of the SPEEK/PTA, SPEEK/$(RSiO_{3/2})_n$/PTA, SPEEK/ZrO_2/PTA and SPEEK/$(RSiO_{3/2})_n$.

As illustrated in Fig. 4a. no sharp peak (and therefore no crystalline structure) can be identified in the WAXS curve of the SPEEK/PTA membrane. This fact is in line with the Guinier analysis of the ASAXS curves, since the PTA anions seem to be homogeneously dissolved by the SPEEK matrix.

Fig. 5 and 6 show the total and separated scattering curves of the SPEEK/ZrO_2/PTA, respectively. Contrary to that described for the SPEEK/PTA membrane, peaks could be seen in the total scattering curves. However, no peak could be seen in the separated scattering curves, suggesting that the peaks are not related to structures containing tungsten. Therefore, the dispersion of the heteropolyacid was not hindered by the presence of the ZrO_2. As reported previously, the ZrO_2 improved the dispersion of the PTA in the SPEK matrix. The same effect seems to take place in the SPEEK/ZrO_2/PTA membrane. The peaks may be caused by ZrO_2 clusters.

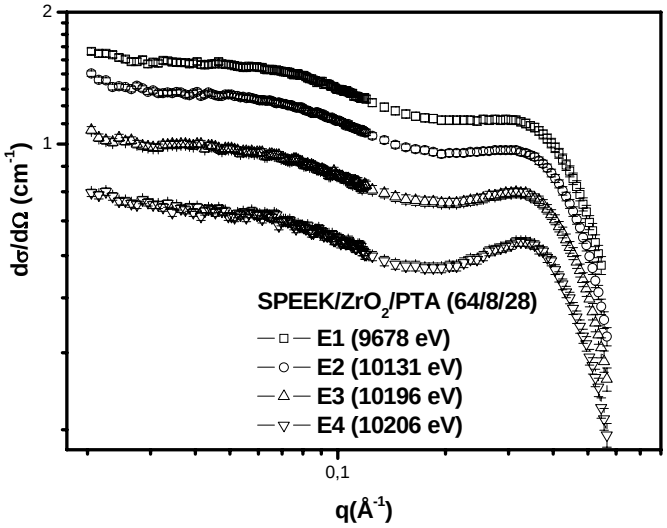

Fig. 5. Total scattering curves of SPEEK/ZrO_2/PTA membranes (64/8/28) obtained at energies closer to the W-L_{III} absorption edge at 10206 eV (see text for details).

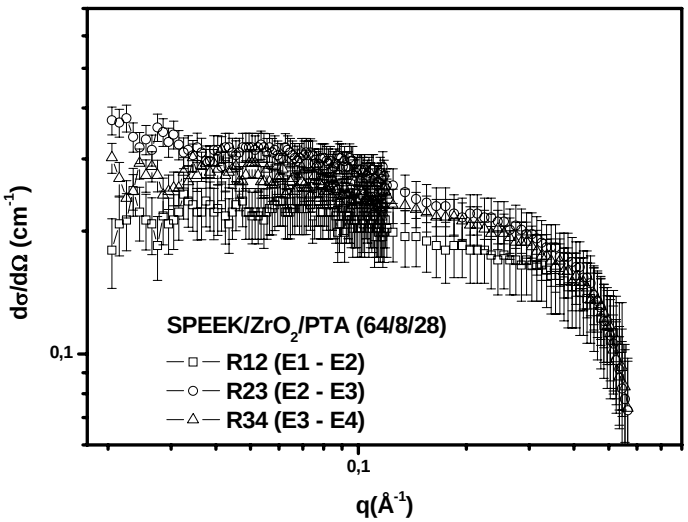

Fig..6. Separated scattering curves produced by SPEEK/ZrO_2/PTA (64/8/28) membrane. These curves were obtained by subtracting the total scattering curve at E1 (9678 eV) from those measured at E4 (10206 eV) or E3 (10196 eV)

The Guinier plots of two separated curves were analyzed as described for the SPEEK/PTA membrane and are displayed in Fig. 7. Values of R and R_g comparable

to the size of the PTA anion were also observed for the SPEEK/ZrO_2/PTA membrane.

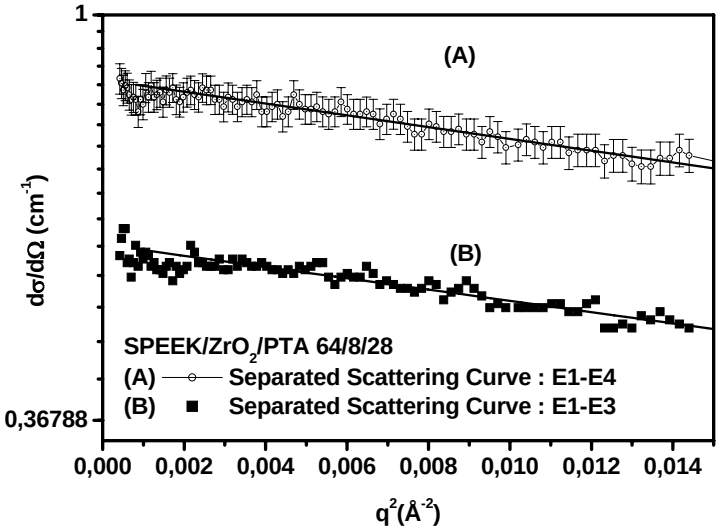

Fig. 7. Guinier plots for SPEEK/ZrO_2/PTA 64/8/28 membranes obtained from the separated scattering curves illustrated in Fig. 6.

Moreover, no crystallization of the PTA was observed, as indicated in Fig. 4b. This fact confirms the hypothesis of a good solubility of PTA in the SPEEK matrix.

The ASAXS curves of the SPEEK/$(RSiO_{3/2})_n$/PTA membrane are displayed in Fig. 8 and Fig. 9. A tremendous increase of the intensity was observed, suggesting the presence of much larger scatterers.

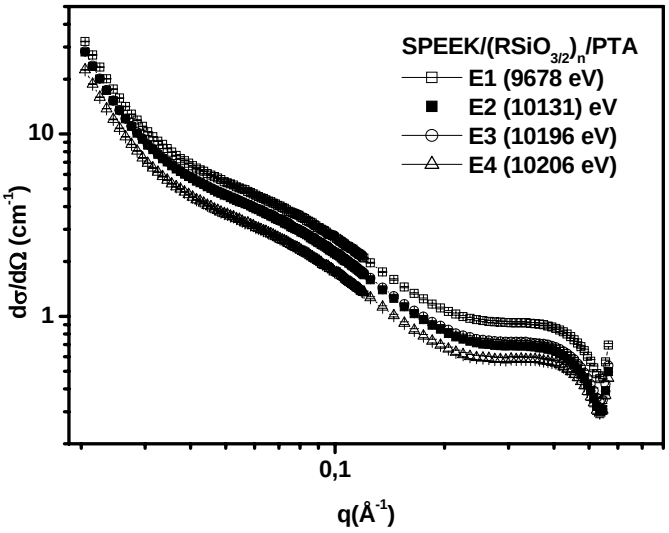

Fig. 8 Total scattering curves of SPEEK/$(RSiO_{3/2})_n$/PTA membrane.

In fact, the separated scattering curves (Fig. 9) are not strictly parallel to each other, and the Guinier analysis could not be applied, since the requirement for the application of the Guinier approximation, equation 4, was not fulfilled . This also shows that the PTA-containing scatters are not isolated particles.

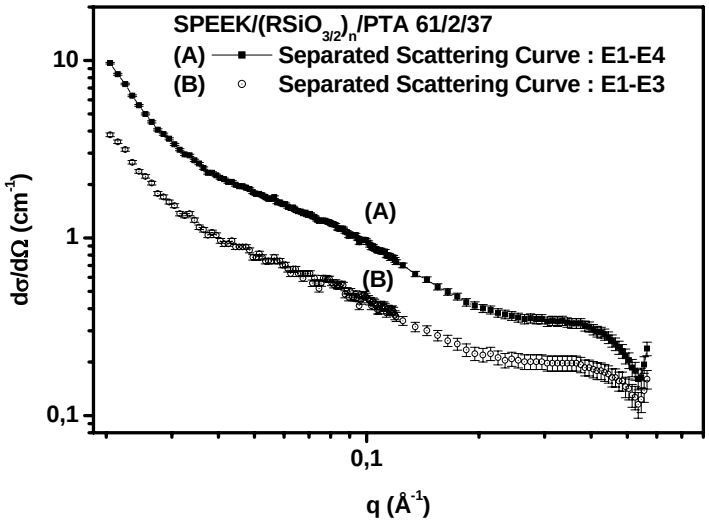

Fig. 9. Separated scattering curves produced by SPEEK/$(RSiO_{3/2})_n$/PTA membrane. These curves were obtained by subtracting the total scattering curve at E1 (9678 eV) from those measured at E4 (10206 eV) or E3 (10196 eV).

The inverse Fourier-transform method was used to analyze the separated scattering curves. For both curves, a distribution of particle radii around 150 Å was found. Therefore, the addition of only 2% poly(3-aminopropyl silsesquioxane) caused an 30-fold increase of the particle size. Although the agglomeration of the PTA particles was observed, as indicated by the noticeable increase of the total scattering and the non-applicability of the Guinier approximation, itt did not lead to crystallization of PTA during the production of the SPEEK/$(RSiO_{3/2})_n$/PTA membrane, as confirmed by the WAXS pattern of this membrane (Fig. 4).

SPEEK/$(RSiO_{3/2})_n$ and SPEEK/ZrO_2 membranes

The SAXS curve of SPEEK/$(RSiO_{3/2})_n$, without heteropolyacids, is reported in Figure 10a. It has a peak at q= 0.255 $Å^{-1}$, indicating that the polysilsesquioxane chains are distributed in particles spaced by the distance of 24.6 Å. Similarly to reported in previous papers from our group, the SAXS curve of SPEEK/ZrO_2 has also a peak centred at q = 0.295 $Å^{-1}$ (Figure 10b), which can also be associated to the presence of ZrO_2 clusters separated by 21.3 Å.

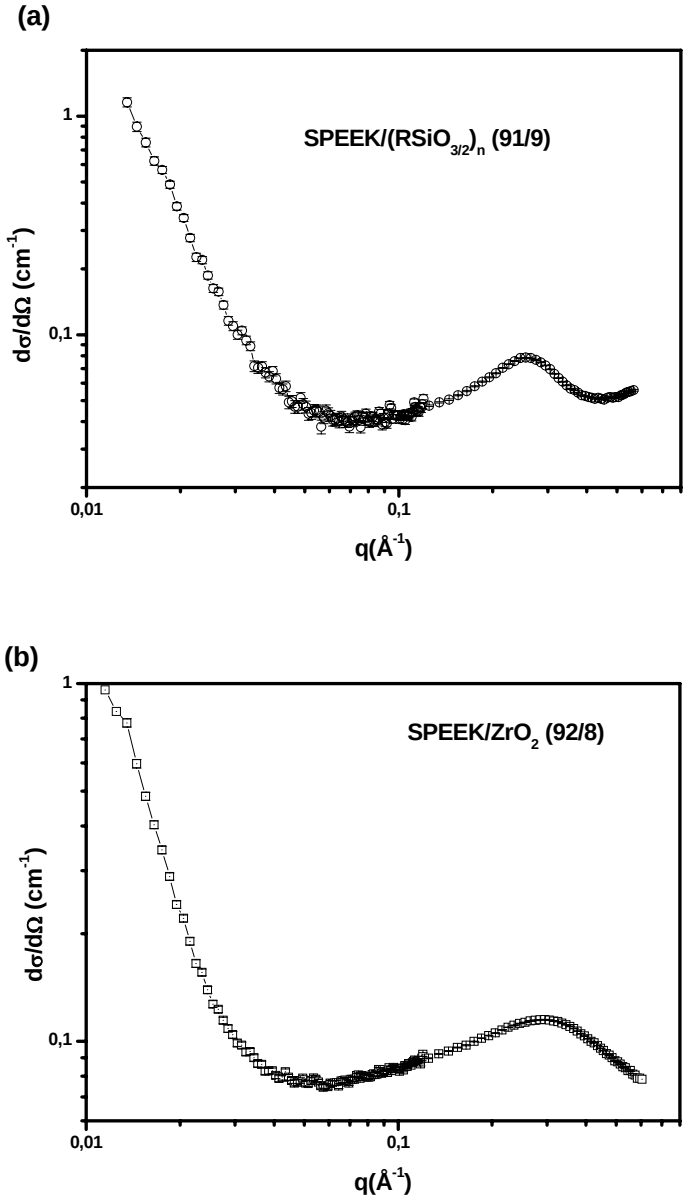

Fig. 10. SAXS curves of SPEEK/$(RSiO_{3/2})_n$ (91/9) (a) and SPEEK/ZrO_2 (92/8) (b) membranes.

5. Discussion

According to the ASAXS and WAXS results, PTA could be homogeneously dispersed in SPEEK matrix. The good compatibility between the heteropolyacid and the polymeric matrix can be explained in term of a compromise between the hydrogen-

bonds between the relative polar groups of the poly(arylene-ether-ether-ketone) back-bone (ether linkages and carbonyl groups), most importantly the pendant –SO_3H groups and the W=O and W-O-H bonds present in PTA, and the very low lattice energy of this heteropolyacid. In order words, these two effects contribute to the dispersion of the highly soluble and hydrophilic PTA as isolated species in the relatively polar and hydrophilic SPEEK matrix.

The ZrO_2 can also interfere in the dispersion of the heteropolyacid in the SPEEK matrix, due to the ability of zirconium oxide to adsorb anions. This effect has been already reported for similar membranes based on sulphonated poly(ether ketone), ZrO_2 and PTA. On its turn, the PTA contributes also for a better dispersion of ZrO_2 in SPEEK, by changing the course of hydrolysis and condensation of zirconium tetrapropylate, during the membrane casting process. The acid nature of phosphotungstic acid favors the formation of more linear structures of oxo-polymers based on Zr-O-Zr bonds.

In fact, the WAXS results do indicate that the ZrO_2 and PTA are dispersed in SPEEK without the formation of crystalline structures of these components. It is hardly possible for the ZrO_2 to crystallize due to the complexation with SPEEK [39] and due to the chemical and physical interactions between ZrO_2 and PTA. Moreover, the PTA has a very low lattice energy and a very high affinity with ZrO_2. Therefore, the phosphotungstic acid would be strongly hindered by these both effects.

Conversely, the amino-functionalized polysilsesquioxane, derived from the hydrolysis and polycondensation of 3-aminopropyltrimethoxysilane during the casting of SPEEK/$(RSiO_{3/2})_n$/PTA membrane, tends to agglomerate the PTA particles, since the

ammonium salts of phosphotungstic acid are much less soluble than the PTA itself. Therefore, the agglomeration of PTA in the presence of the poly(3-aminopropyl silsesquioxane) is basically due to the precipitation of the phosphotungstate anions by the $–NH_2$ groups, from the polysilsesquioxane component. The precipitation of PTA as “ammonium salt” did not favoured the crystallization of this heteropolyacid. As illustrated by Fig. 4b, no crystalline phase of PTA could be identified in the WAXS pattern of SPEEK/$(RSiO_{3/2})_n$/PTA membrane. This can be also explained in terms of disordered structures imposed by the presence of the poy(3-aminopropyl silsesquioxane) chain in between the PTA anions, which hinder the formation of a crystalline lattice.

6. Conclusion

ASAXS and SAXS/WAXS studies on SPEEK membranes containing phosphotungstic acid revealed that the distribution of this heteropolyacid in SPEEK was homogeneous, since the acid could be dissolved in the polymer matrix almost at the molecular level. The use of in-situ generated poly(3-aminopropyl silsesquioxane), in order to reduce the PTA bleeding-out, caused the agglomeration of the heteropolyacid in larger structures, although no crystallisation could be detected by WAXS at all. Conversely, the presence of in-situ generated ZrO_2 nanoparticles did not have any effect on the distribution of PTA on SPEEK.

References

[1] T. Bock, H. Mohwald, R Mülhaupt, Macromol. Chem. Phys. 208 (2007) 1324.

[2] H. Steininger, M. Schuster, K. D. Kreuer, A. Kaltbeitzel, B. Bingöl, W. H. Meyer, S. Schauff, G. Brunklaus, J. Maier, H. W. Spiess, Phys. Chem. Chem. Phys. 9 (2007) 1764.

[3] N. W. Deluca, Y. A. Elabd, J. Polym. Chem., Polym. Phys. Ed. 44 (2006) 2201.

[4] D. Gomes, J. Roeder, M. L. Ponce, S. P. Nunes, J. Membrane Sci.295 (2007) 121.

[5] S. Vetter, V. Abetz, G. Goerigk, I. Büder, S. P. Nunes, Desalination 199 (2006)

[6] E. Parcero, R. Herrera, S. P. Nunes, J. Membrane Sci. 285 (2006) 206.

[7} P. Xing, G. P. Robertson, M. D. Guiver, S. D. Mikhailenko, S. Kaliaguine, Polymer 46 (2005) 3257.

[8] S. Vetter, S. P. Nunes, React. Fun. Polym. 61 (2004) 171.

[9] P. Xing, G. P. Robertson, M. D. Guiver, S. D. Mikhailenko, K. Wang, S. Kaliaguine, J. Membrane Sci. 229 (2004) 95.

[10] K. Jakoby, K. V. Peinemann, S. P. Nunes, Macromol. Chem. Phys. 204 (2003) 61.

[11] A. Dyck, D. Fritsch, S. P. Nunes, J. Appl. Polym. Sci. 86 (2002) 2820.

[12] S. Liu, T. Chen, Polymer 42 (2001) 3293.

[13] B. Smitha, S Sridhar, A. A. Khan, J. Polym. Sci. Polym. Phys. Ed. 43 (2005) 1538.

[14] M. L. Ponce, L. A. S. A. Prado, V. Silva, S. P. Nunes, Desalination 162 (2004) 383.

[15] M. L. Ponce, L. Prado, B. Ruffmann, K. Richau, R. Mohr, S. P. Nunes, J. Membrane Sci. 217 (2003) 5.

[16] S. M. J. Zaidi, S. D. Mikhailenko, G. P. Robertson, M. D. Guiver, S. Kaliaguine, J. Membrane Sci. 173 (2000) 17.

[17] V. S. Silva, S. Weisshaar, R. Reissner, B. Ruffmann, S. Vetter, A. Mendes, L. M. Madeira, S. Nunes, J. Power Sources 145 (2005) 485.

[18] M. L. Hill, Y. S. Kim, B. R. Einsla, J. E. McGrath, J. Membrane Sci. 283 (2006) 102.

[19] M. H. Woo, O. Kwon, S. H. Choi, M. Z. Hong, H. W. Ha, K. Kim, Eletrochim. Acta 51 (2006) 6051.

[20] S. P. Nunes, B. Ruffmann, E. Rikowski, S. Vetter, K. Richau, J. Membrane Sci. 203 (2002) 215.

[21] J. A. Asensio, P. Gomez-Romero, Fuel Cells 5 (2005) 336.

[22] J. A. Asensio, P. Gomez-Romero, S. Borros, Eletrochim. Acta 50 (2005) 4715.

[23] Z. Wang, H. Ni, C. Zhao, X. Li, T. Fu, H. Na, J. Polym. Sci. Polym. Phys. Ed. 44 (2006) 1967.

[24] L. A. S. A. Prado, G. Goerigk, M. L. Ponce, K. Schulte, V. M. Garamus, R. Willumeit, S. P. Nunes, J. Polym. Sci. Polym. Phys. Ed. 43 (2005) 2981.

[25] L. A. S. A. Prado, M. L. Ponce, S. S. Funari, K. Schulte, V. M. Garamus, R. Willumeit, S. P. Nunes, J. Non-Cryst. Solids 351 (2005) 2194

[26] L. A. S. A. Prado, H. Wittich, K. Schulte, G. Goerigk, V. M. Garamus, R. Willumeit, S. Vetter, B. Ruffmann, S. P. Nunes, J. Polym. Sci. Polym. Phys. Ed. 42 (2004) 567.

[27] A. Bota, Z. Varga, G. Goerigk, J. Appl. Cryst. 40 (2007) 259.

[28] U. Vainio, K. Pirkkalainen, K. Kisko, G. Goerigk, N. E. Kotelnikova, R. Serimaa, Eur. Phys. J. D. 42 (2007) 93.

[29] R. Schweins, G. Goerigk, K. Huber, Eur. Phys. J. E. 21 (2006) 99.

[30] G. Goerigk, D. L. Willianson, J. Appl. Phys. 99 (2006)

[31] D. Tatchev, G. Goerigk, E. Valova, J. Dille, R. Kranold, S. Armyanov, J. L. Delplancke, J. Appl. Cryst. 38 (2005) 787.

[32] R. A. Register, S. L. Cooper, Macromolecules 23 (1990) 318.

[33] Y. S. Ding, S. R. Hubbard, K. O. Hodgson, R. A. Register, S. L. Cooper, Macromolecules 21 (1988) 1698.

[34] Q. de Robillard, X. Guo, N. Dingenouts, M. Ballauff, G. Goerigk, Macromol. Symp. 164 (2002) 81.

[35] A. Guinier; G. Fournet in Small-Angle Scattering of X-Rays: John Willey & Sons, Inc. 1955; pp. 126-128.

[36] H.-G. Haubold, K. Grünhagen. M. Wagener, H. Jungbluth, H. Heer, A. Pfeil, H. Rongen, G. Brandenburg, R.Moeller, J. Matzerath, P. Hiller, H. Halling, Rev Sci Instrum 60 (1989) 1943.

[37] B. D. Grady, E. M. O'Connell, C. Z. Yang, S. L. Cooper, J Polym Sci, Part B: Polym Phys 32 (1994) 2357.

[38] M. Yoshimune, Y. Yoshinaga, T. Okuhara, Microp Mesop Mater 51 (2002) 165.

[39] A. Lorenz, G. Kickelbick, U. Schubert, Chem Mater 9 (1997) 2551.